# Accepted Manuscript

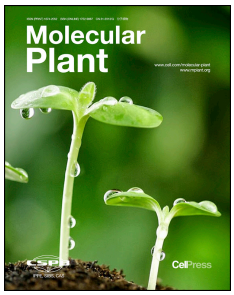


TRICHOME AND ARTEMISININ REGULATOR 1 Is Required for Trichome Development and Artemisinin Biosynthesis in Artemisia annua L

Hexin Tan, Ling Xiao, Shouhong Gao, Qing Li, Junfeng Chen, Ying Xiao, Qian Ji, Ruibing Chen, Wansheng Chen, Lei Zhang

PII: S1674-2052(15)00199-9

DOI: 10.1016/j.molp.2015.04.002

Reference: MOLP 120

To appear in: *MOLECULAR PLANT*

Received Date: 26 January 2015

Revised Date: 4 April 2015

Accepted Date: 6 April 2015

Please cite this article as: **Tan H., Xiao L., Gao S., Li Q., Chen J., Xiao Y., Ji Q., Chen R., Chen W., and Zhang L.** (2015). TRICHOME AND ARTEMISININ REGULATOR 1 Is Required for Trichome Development and Artemisinin Biosynthesis in Artemisia annua L. Mol. Plant. doi: 10.1016/j.molp.2015.04.002.

# *TRICHOME AND ARTEMISININ REGULATOR* 1 Is Required for Trichome Development and Artemisinin Biosynthesis in *Artemisia annua* L.

Hexin Tan[a, 1], Ling Xiao [a, 1], Shouhong Gao[b], Qing Li[b], Junfeng Chen[b], Ying Xiao[b], Qian Ji[a], Ruibing Chen[a], Wansheng Chen[b], Lei Zhang [a *]

[a] Department of Pharmaceutical Botany, School of Pharmacy, Second Military Medical University, Shanghai 200433, China

[b] Department of Pharmacy, Changzheng Hospital, Second Military Medical University, Shanghai 200003, China

* Corresponding author: E-mail: zhanglei@smmu.edu.cn

[1] These authors contributed equally to this work.

**Running title:** TAR1 regulates artemisinin and trichome formation

**Short Summary:**

TAR1, an AP2 transcription factor, controls the development of trichomes and the biosynthesis of artemisinin in *A. annua*. RNA interference of *TAR1* in *A. annua* caused a decreased accumulation of artemisinin, abnormal phenotype of Glandular secreting trichomes and non-glandular trichomes, as well as altered cuticular wax load. *TAR1* is involved in a crucial regulation network controlling the biosynthesis of artemisinin by regulating *CYP71AV1* and *ADS*, two key enzyme genes in the biosynthesis pathway of artemisinin.

## ABSTRACT

Trichomes, small protrusions on the surface of many plants, can produce and store various secondary metabolic products. Artemisinin, a famous and potent medicine for malaria, is synthesized, stored and secreted by *Artemisia annua* trichomes. However the molecular basis regulating the biosynthesis of artemisinin and the development of trichomes remains poorly understood. Here, we revealed the crucial role of an AP2 transcription factor, TRICHOME AND ARTEMISININ REGULATOR 1 (TAR1), in controlling the development of trichomes and the biosynthesis of artemisinin in *A. annua*. *TAR1* is expressed mainly in young leaves, flower buds, and some trichomes, and its protein is specially located in cell nucleus. In *TAR1-RNAi* lines, the phenotype of trichomes and the composition of cuticular wax were altered. The content of artemisinin was dramatically reduced as well, which increased significantly when *TAR1* was overexpressed. Furthermore, the expression of many genes that participate in artemisinin biosynthesis was changed when *TAR1* was silenced or overexpressed, especially *ADS* and *CYP71AV1*, which were shown to be the likely direct targets of *TAR1* through electrophoretic mobility shift, yeast one-hybrid and transient transformation GUS assay. These results indicate that *TAR1* is a key component of the molecular network regulating *A. annua* trichome development and artemisinin biosynthesis.

**Key words**: *Artemisia annua*; Artemisinin; Trichome; AP2 transcription factor; Wax.

## INTRODUCTION

Artemisinin, a sesquiterpene lactone with an endoperoxide bridge, was first isolated from *Artemisia annua* L. (sweet wormwood). Artemisinin and its derivatives have widespread medicinal values and have been shown to be effective in the treatment of cancer, viral infections and autoimmune diseases (Wang et al., 2007; Efferth et al., 2008; Crespo-Ortiz and Wei, 2012). Furthermore, artemisinin is the key ingredient of

front-line antimalarial drugs (Noorden, 2010), and artemisinin-based combination therapies (ACTs) are recommended by the World Health Organization (WHO) as the first-line treatment for uncomplicated *P. falciparum* malaria (WHO, 2014). Despite the confirmed medicinal value of artemisinin, little is known concerning the regulatory mechanism by which the trichomes of *A. annua* develop and artemisinin is synthesized.

Trichomes are small protrusions of epidermal origin on the surfaces of leaves and other organs of many plants. There are two kinds of trichomes, named Glandular secreting trichomes (GSTs) and T-shaped non-glandular trichomes (TNGs) in *A. annua* (Ferreira and Janick, 1995), however GSTs do not exist in *Arabidopsis thaliana*. One of the most remarkable features of trichomes is their capacity to synthesize, store and sometimes secrete large amounts of specialized metabolites (Schilmiller et al., 2008). For example, in Humulus lupulus, GSTs are the cell factories of branched-chain amino acids (BCAAs) degradation and bitter acid biosynthesis (Xu et al., 2013). Within *A. annua*, GSTs (*Aa*GSTs) are the sites for producing and storing of artemisinin (Duke and Paul, 1993; Duke et al., 1994). *Aa*GSTs are a 10-celled biseriate translucent structure of two stalk cells, two basal cells, four sub-apical cells and two apical cells (Olsson et al. , 2009). It has been shown that artemisinin biosynthesis takes place in both apical and sub-apical cells (Olofsson et al., 2012; Soetaert et al., 2013). TNGs, with filamentous five-celled T-trichomes, have long been thought of as physical barriers of plants. Very recently, they have been confirmed to have specific genes expression in sesquiterpenoid and triterpenoid biosynthesis pathways (Soetaert et al. , 2013). However, the regulating mechanism is largely unknown underlying the development of trichomes especially GSTs.

The production and storage of artemisinin take place in *Aa*GSTs (Duke and Paul, 1993; Duke et al., 1994). The compound originates from isopentenyl diphosphate (IPP) which comes from either mevalonate (MVA) pathway or methylerythritol phosphate (MEP) pathway (Covello, 2008). Recently, the identification of several enzymes, such as Amorpha-4,11-diene synthase (ADS), Cytochrome P450 monooxygenase (CYP71AV1), Cytochrome P450 reductase (CPR), Alcohol dehydrogenase 1 (ADH1),

Artemisinic aldehyde delta-11(13) reductase (DBR2) and Aldehyde dehydrogenase (ALDH1), has revealed the potential mechanisms responsible for artemisinin biosynthesis. The first specialized step toward artemisinin biosynthesis is the cyclization of farnesyl pyrophosphate (FPP) to amorpha-4, 11-diene by ADS (Nguyen et al., 2011). Then, amorpha-4, 11-diene is oxidized thrice to form artemisinic alcohol (AAOH), artemisinic aldehyde (AAA) and artemisinic acid (AA) respectively by CYP71AV1 (Teoh et al., 2006; Wang et al., 2011). DBR2 catalyzes AAA to form dihydroartemisinic aldehyde (DHAAA) (Wu et al., 2012), and ALDH1 converts DHAAA to dihydroartemisinic acid (DHAA) (Teoh et al., 2009). Most of these enzymes are specifically localized in *Aa*GSTs (Olsson et al., 2009; Wang et al., 2013).

The APETALA2/ethylene response factor (AP2/ERF) transcription factors (TFs) belong to one of the largest plant TF families, and are characterized by conserved AP2/ERF DNA binding domains of 57–66 amino acids in size (Okamuro et al., 1997). The AP2/ERF genes constitute a large multigene family divided into four subfamilies, named AP2, CBF/DREB, ERF, and RAV, based on their sequence similarities and numbers of AP2/ERF domains (Sakuma et al., 2002). Members of AP2/ERF TFs function as key regulators in plant metabolism, development and adaptive responses to environmental stimuli (Licausi et al., 2013). In Arabidopsis, AP2/ERF TFs *WAX INDUCER1*/*SHINE1* coordinate with MIXTA-Like TFs in order to regulate the biosynthesis of waxy substances and cuticle development (Oshima et al., 2013), and the SHINE clade of AP2 domain TFs alters cuticle properties and trichome branch development (Aharoni et al., 2004). The Arabidopsis *shine* gain-of-function mutant and plants over expressing *WIN1/SHN1*, *SHN2*, or *SHN3* have increased the accumulation of epidermal wax, ectopic wax crystals in leaves, and increased the expression of genes involved in wax biosynthesis, including *ECERIFERUM1* (*CER1*), *3-KETOACYLCOA SYNTHASE1* (KCS1), and *CER2* (Aharoni et al., 2004; Broun et al., 2004).

In *A. annua*, molecular biology studies have identified a number of genes that control the biosynthesis of artemisinin. For example, AaORA, a trichome-specific AP2/ERF TF, is a positive regulator of artemisinin biosynthesis and also increases

resistance to *Botrytis cinerea* (Lu et al., 2013). Furthermore, two jasmonate-responsive AP2/ERF TFs (AaERF1 and AaERF2) are able to bind to the cis-elements both in *ADS* and *CYP71AV1* promoters, which results in an increase in artemisinin accumulation (Yu et al., 2012). Finally, AabZIP1, a basic leucine zipper TF, connects ABA signaling with artemisinin biosynthesis through the activation of *ADS* and *CYP71AV1* expression in *A. annua* (zhang et al., 2015). Although there is good working knowledge of the genes that control the biosynthesis of artemisinin, little is known about the genetic mechanisms that regulate the development of the specialized trichomes that produce and store artemisinin in *A. annua*.

In this study, we describe the critical role of an AP2/ERF TF, TAR1, in the development of trichomes and the biosynthesis of artemisinin in *A. annua*. TAR1 is mainly expressed in young leaves and flower buds, and is specially localized within the cell nucleus. Importantly, we found that RNA interference (RNAi) of *TAR1* in plants caused a decreased accumulation of artemisinin, abnormal phenotype of *Aa*GSTs and TNGs, as well as altered cuticular wax load. Interestingly, the content of artemisinin increased markedly in *TAR1* overexpressed transgenic *A. annua* lines and the expression of key enzyme genes also elevated dramaticlly, suggesting that *TAR1* was probably involved in the crucial regulation network controlling the biosynthesis of artemisinin. Furthermore, using electrophoretic mobility shift assay (EMSA), we've shown that *TAR1* is able to bind to the cis-elements of *ADS* and *CYP71AV1* promoters, two important genes in the biosynthesis pathway of artemisinin. These results provide important insights into the crucial role of TAR1 in a transcriptional regulatory network for artemisinin biosynthesis and trichome development.

## RESULTS

### Isolation of *TAR1* Gene from *A. annua* and the Sequence Analysis

In order to identify the potential genes responsible for the development of trichomes or the biosynthesis of artemisinin in *A. annua*, we searched the transcriptome sequencing database at National Center for Biotechnology Information (NCBI). Graham et al. (2010) predicted seven genes may participate in the development of

trichome by using the TBLASTN algorithm. *TAR1* (EZ159016), an AP2/ERF family TF, was one of the 7 genes. To clone *TAR1*, the cDNA was reverse transcripted using the leaves of *A. annua* as the source of mRNA. The *TAR1* transcript is 1043 bp in length and contains an open reading frame (ORF) of 543 bp with a 290 bp intron, a 206 bp 5'untranslated region (UTR) and a 294 bp 3'UTR (Figure 1A ). The TAR1 ORF encodes a putative AP2/ERF protein of 180 amino acids with an AP2 domain between the 5th and 68th amino acids (Figure 1A).

To determine the subcellular localization of TAR1, we constructed a translation fusion between the cDNA for the green fluorescent protein (GFP) and the full-length TAR1 coding region. The TAR1-GFP fusion construct and the GFP alone control, both driven by the 35S promoter, were introduced into protoplasts isolated from etiolated rice stems. As expected, the free GFP was found in the cytoplasm (Figure 1B). By contrast, the TAR1-GFP fusion protein was observed exclusively in the nucleus (Figure 1C-1E). These results suggest that TAR1 is localized to the nucleus.

To gain additional insights into the phylogenetic relationship between TAR1 and its close homologs, we searched public databases using BLAST with the TAR1 sequence as a query. The full-length amino acid sequences of TAR1 and its 20 closest homologs, including *AtWIN1*, *AtSHINE3*, two known genes from Arabidopsis, as well as three AP2 TFs, which had been reported from *A. annua*, were used for phylogenetic analysis. Our results revealed that TAR1 had homologs in many species and AtWIN1, AtSHINE3 seemed to be its orthologous genes in Arabidopsis (Figure 1F). Furthermore, sequence comparison indicated that TAR1 shared 67% and 58% overall identity with AtWIN1, AtSHINE3 respectively (Figure 1G). In Arabidopsis, *WIN1*/*SHN1* was a transcriptional activator of epidermal wax accumulation (Broun et al., 2004). Furthermore, the Arabidopsis *shine* gain-of-function mutant and plants over expressing *WIN1/SHN1*, *SHN2*, or *SHN3* have increased the accumulation of epidermal wax and ectopic wax crystals in leaves, as well as defective TNG branches (Aharoni et al., 2004; Broun et al., 2004). In *TAR1* RNAi transgentic lines, the cuticular wax was altered as well. However, the biosynthesis of artemisinin and the development of GSTs were not analyzed in Arabidopsis. Additionally, the *A. annua*

*AaORA*, *AaERF1* and *AaERF2* gene also encodes AP2 protein, which plays major roles in the biosynthesis of artemisinin (Lu et al., 2013). Comparative analysis revealed that their genetic relationships were far from *TAR1* (Figure 1F, Supplemental Figure 1).

### *TAR1* Is Mainly Expressed in Young Leaves and Flower Buds

To understand the function of *TAR1*, we analyzed the expression pattern of *TAR1*. Total RNAs were isolated from different organs of *A. annua* (root, stem, old leaf, young leaf, very young flower bud, flower bud and flower), and reverse transcription (RT)-PCR, quantitative RT-PCR (qRT-PCR) analyses showed that *TAR1* expression was detectable in stem, leaf, bud and flower, high at young leaf and bud, but was not detectable in root (Figure 2A, 2B). To dissect the detailed expression of *TAR1*, we analyzed its transcript level in leaves at different positions by RT-PCR and qRT-PCR. These results showed that *TAR1* was expressed highly within young leaves (L1 and L2), and declined as grew (Figure 2C-2E).

To determine the spatial and temporal expression patterns of *TAR1* more precisely, we transformed a *pTAR1-GUS* (β-glucuronidase) fusion construct (for expression of the GUS marker protein driven by the 1360-bp *TAR1* promoter region (Supplemental Figure 2) into the wild type *A. annua*. Histochemical GUS staining of transgenic lines containing *pTAR1-GUS* showed that GUS activity was detectable in young leaves, especially in the tender tip part, and reached the maximum level at apical meristem (Figure 2F, 2G), while no obvious signal was detected in wild-type *A. annua* control(Figure 2H). Interestingly, GUS activity was also detected in TNGs and some GSTs, in 10 cells or in two stalk cells and two basal cells at the bottom (Figure 2I-2L). Furthermore, GUS activity was detectable in young buds at the flowering stage (Figure 2M), which correlated well with the RT-PCR results. No obvious signal was detected in the wild-type control (Figure 2N), proving the specificity of this experiment.

### TAR1 Protein Is Localized to the Cell Nucleus of Young Leaves

Like other TFs, TAR1 was predicted to localize to the cell nucleus by programs such

as PSORT (http://psort.hgc.jp/form.html) and SubLoc v1.0 (http://www.bioinfo.tsinghua.edu.cn/SubLoc/eu_predict.htm), and TAR1 had been proved to be localized to the nucleus of rice protoplasts by transient expression experiment (Figure 1B-1E). To understand the *in vivo* localization of TAR1, we made a translational fusion between the full length *TAR1* coding region and *GFP* under the control of the *TAR1* native promoter (*pTAR1:TAR1-GFP*) (Figure 3 A). In agreement with data from the *TAR1* mRNA analysis, the wild-type transgenic plants expressing *pTAR1:TAR1-GFP* displayed GFP fluorescence signal specifically within young leaf cell nucleus, which was further confirmed by 4′,6-diamidino-2-phenylindole (DAPI) staining (Figure 3B-3F). No GFP fluorescence signal was detected in the wild-type control (Figure 3G-3K), proving the specificity of this experiment. These results suggest that the TAR1 protein is specifically located in the nucleus of young *A. annua* leaf cells, which correlates well with the expression pattern of its gene.

**Silencing of *TAR1* in *A. annua* Reduces Artemisinin Production and Overexpression of *TAR1* Increases Artemisinin Yield**

To characterize the biological role of *TAR1* in *A. annua*, we used RNAi. The *1300-pHANNIBAL-TAR1-RNAi* construct used a 414-bp *TAR1* cDNA fragment including 54-bp 3′ untranslated region, which has a low similarity to other sequences in *A. annua* (Figure 4A), and this construct was introduced into *A. annua* leaf explants by *Agrobacterium tumefaciens* EHA105. Transgenic plants were screened in a hygromycin-containing medium and were further confirmed by genomic PCR using the primers provided in Supplemental Table 1 (Supplemental Figure 3). Nineteen independent $T_0$ transformant lines were obtained and reduction of *TAR1* expression was confirmed by semiquantitative RT-PCR in all lines (Supplemental Figure 4A). Seven independent transgenic lines were chosen for qRT-PCR analysis，and the transcript levels of *TAR1* were decreased by 28%-53% compared with negative control lines transformed with the empty vector (Supplemental Figure 4B). In addition, the level of artemisinin, DHAA and AA were tested in the RNAi transgenic plants. The leaves of vegetative development stage and buds of reproductive development

stage, where the expression of *TAR1* gene is high, were extracted by ethanol and analyzed by LC-MS/MS. Compared with negative control lines transformed with the empty vector, the levels of artemisinin, AA and DHAA in *TAR1-RNAi* plants reduced 39-64%, 45-75% and 33-72%, respectively (Figure 4B, 4C, Supplemental Figure 5). These results led us to the conclusion that silencing of *TAR1* reduces the production of artemisinin, AA and DHAA, and that *TAR1* is involved in controlling the biosynthesis of artemisinin.

To further verify the biological role of *TAR1* in the biosynthesis pathway of artemisinin, *TAR1* driven by double *CaMV35S* promoter, was overexpressed in *A. annua*. Twenty independent positive $T_0$ transformant lines were obtained and the expression of *TAR1* increased very significantly by 12 to 23 folds according to qRT-PCR results (Supplemental Figure 4C). As expected, the levels of artemisinin, DHAA and AA were increased by 22%-38%, 69%-130% and 28%-164% respectively in leaves, and 34%-57%, 22%-79%, 12%-61% respectively in flower buds (Figure 4D). These results demonstrate that *TAR1* is an important positive regulator in the biosynthesis pathway of artemisinin and may well be used for engineering artemisinin biosynthesis in *A. annua*.

**Silencing of *TAR1* Causes Abnormal Trichome Development**

Production of artemisinin relies on the normal development and formation of its specialized producer organ GST trichomes. To further understand the biological role of *TAR1* in this process, we characterized the morphology of wild-type and *TAR1-RNAi* plants using leaves of the same vegetative development stage, and found defects of both GSTs and TNGs on the surface of transgenic *A. annua* leaf, while the density of trichome didn't have an obvious change. We treated young leaves with 75% alcohol to extract chlorophyll and got distinct trichome, and found that the chlorophyll of *TAR1-RNAi* plants was easier to be extracted (Figure 5A-5C). Under microscope, different from the regular and oval GSTs of wild-type *A. annua* leaf (Figure 5A，red arrow), most GSTs of *TAR1-RNAi* plants were abnormal (Figure 5B，5C, blue arrow). To determine the trichome morphological defects in the *TAR1-RNAi*

plants, leaves were treated with phosphate buffer overnight, then decolorized by 75% alcohol and pressed by glass slide. 10-celled biseriate translucent GSTs could be clearly found on the wild-type leaf (Figure 5D), but a large amount of *Aa*GSTs of *TAR1-RNAi* plants exhibited different phenotype with an abnormal inflated top and reduced number of cells (Figure 5E, 5F).

Under fluorescence microscopy, the strong red autofluorescence of chlorophyll, and green autofluorescence of *Aa*GSTs, shown by white arrows, could be obviously detected on wild-type leaf (Figure 5G, 5H). By contrast, the autofluorescence of many GSTs on *TAR1-RNAi* plants leaf was very weak, shown by blue arrows, indicating defective *Aa*GSTs (Figure 5I, 5K, 5J, 5L). Moreover, there was a very strong yellow autofluorescence of the *TAR1-RNAi* leaf (Figure 5I, 5K, 5J, 5L), indicating that the surface of *TAR1-RNAi* leaf was deficient too. In addition, different from the wild-type TNGs (shown by black arrows in Figure 5H), the TNGs of *TAR1-RNAi* lines were filiform (Figure 5L).

To obtain a more detailed understanding of the abnormalities of TNGs development in *TAR1-RNAi* plants, scanning electron microscope (SEM) was performed. In accordance with the light microscopy, the TNGs of *TAR1-RNAi* lines were abnormally extended, distorted and formed a reticular structure, very different from the wild-type TNGs (Figure 6A-6F). These results prove that TAR1 is required for the development of both GSTs and TNGs in *A. annua*.

**Silencing of *TAR1* Alters the Wax Load and Cuticle Permeability**

When doing morphologic observations, we found that the chlorophyll of *TAR1-RNAi* was easier to be extracted by alcohol (Figure 5A-5C), consistent with the mutant of its homologous gene in Arabidopsis (Aharoni et al., 2004). Futhermore, the unusual yellow autofluorescence of *TAR1-RNAi* leaves together indicated a defect of the leaf surface (Figure 5I, 5K, 5J, 5L). We used SEM for a detailed comparison between the surfaces of wild-type *A. annua* leaf and those of *TAR1-RNAi* lines, and found that the surface of *TAR1-RNAi* adaxial side leaf was covered with abnormal wax deposition, whereas wild-type surface was smooth and showed only little wax deposition (Figure

6G, 6H). To investigate whether the cuticular membrane properties of *TAR1-RNAi* leaf were altered in detail, we conducted chlorophyll leaching experiment in which leaves of the same vegetative period from both *TAR1-RNAi A. annua* and empty vector transgenic plants were submerged in 80% ethanol for different time periods, and the chlorophyll concentration in the solution was determined. Chlorophyll was extracted much faster from leaves of *TAR1-RNAi* compared with the empty vector control (Figures 7A and 7B); therefore, the higher elution of chlorophyll from *TAR1-RNAi* leaves indicates an increase in cuticle permeability.

The abnormal wax deposition on the surface of *TAR1-RNAi* leaves and increased cuticle permeability indicate defects in the synthesis of aliphatic components. To test this hypothesis, we conducted a detailed chemical analysis of chloroform extractable cuticular waxes as well as aliphatic cutin monomers and total soluble lipids from wild-type and *TAR1-RNAi* leaves by gas chromatography–mass spectrometry (GC-MS) (Broun et al. , 2004). Total wax of *TAR1-RNAi* leaves (average, 6.35 mg/g) decreased by 25.67% compared with the wild type (average, 8.55 mg/g; $P < 0.05$) (Table 1). Analytical results showed that the wax of wild-type leaf contained primary alcohols and esters (from the acyl reduction pathway) as well as alkanes (from the decarbonylation pathway). In sharp contrast, the wax of *TAR1-RNAi* lines exhibited a different composition. Total primary alcohols and esters were reduced by 16.05% and 19.94%, and total alkanes were decreased by 28.32% ($P<0.01$). Total fatty acids and terpenes were reduced by 23.20% ($P<0.05$) and 8.90% in the *TAR1*-RNAi line wax mixture, respectively (Table 1).

In wild-type and *TAR1-RNAi* leaf waxes, primary alcohols, fatty acids and alkanes were dominated by constituents with even carbon numbers (Figure 7C-7E, Supplemental Figure 6). A significant decrease in the levels of C24 ($P < 0.01$) and C26 ($P < 0.05$) primary alcohols (Figure 7C), as well as C16 ($P < 0.05$), C18 ($P < 0.05$), C20 fatty acid and C22 dioic fatty acid ($P < 0.01$) (Figure 7D) were observed in *TAR1-RNAi* lines. In addition, alkenes (C17, C18, C20 and C21) also decreased in the mutant ($P < 0.01$ for C17, C18 and C20; $P < 0.05$ for C21) (Figure 7E). The wax mixture showed chain length distributions dominated by C26/C28 for primary

alcohols, by C16/C18 for fatty acids and by C16/C17/C18/C21/C26 for alkanes, which was similar to the wild type. These results suggest that *TAR1* is required for the normal accumulation of cuticular wax on the surface, which is crucial for the development of both GSTs and TNGs.

Furthermore, two cuticular triterpenoids, β-amyrone and α-amyrone, were identified in *TAR1-RNAi* lines. Compared with control plants, the accumulation of α-amyrone was decreased in *TAR1*- silenced plants, while β-amyrone was increased (Figure 7F).

To elucidate the possible mechanism of the metabolite content change, we detected the expression of wax related genes including *TFAR* (trichome-specific fatty acyl-CoA reductase 1), *OSC2* (oxidosqualene cyclase) and *CYP716A14v2* (cytochrome P450-dependent monooxygenases) by qRT-PCR. *TFAR1* catalyzed the formation of C24 and C26 fatty alcohols (Maes et al., 2011). *OSC2* and *CYP716A14v2* were involved in the biosynthesis of amyrone (Moses et al., 2015). qRT-PCR results showed a decreased transcript levels of *TFAR* and *CYP716A14v2* and an increased transcript of *OSC2* in *TAR1*- silenced plants (Figure 7G). The expression change of wax related genes further confirmed the alteration of wax load.

**TAR1 Interacts with ADS and CYP71AV1 Two Key Enzymes in Artemisinin Synthesis**

To explore the function of TAR1, we measured the content of artemisinin, AA and DHAA in *TAR1-RNAi*, *TAR1*-Overexpression (OX) and wild-type *A. annua*, and found that the levels of artemisinin, AA and DHAA all decreased both in leaves of vegetative development stage and flower buds in *TAR1-RNAi* lines. Conversely, the levels of artemisinin, AA and DHAA increased in *TAR1*-OX lines (Figures 4). To explore the regulatory mechanism of TAR1 in the biosynthesis of artemisinin, the expression of enzyme genes involved in artemisnin biosynthesis were analyzed by qRT-PCR in wild-type, *TAR1*-OX and *TAR1-RNAi A. annua* lines (Figure 8A, 8B). The general mevalonate (MVA) or methylerythritol phosphate (MEP) pathway enzymes including 3-hydroxy-3-methylglutaryl coenzyme A reductase (HMGR),

1-deoxyxylulose 5-phosphate synthase (DXS), 1-deoxyxylulose 5-phosphate reductoisomerase (DXR), farnesyl diphosphate synthase (FPS), as well as the artemisinin pathway enzymes of DBR2, CPR, ADS and CYP71AV1 were analyzed for their expressions in *TAR1-RNAi* plants (Figure 8A, 8C). qRT-PCR analysis indicated that in *TAR1-RNAi* lines the expressions of *DXS* and *DXR*, which located in upstream MEP pathway, were increased compared to the control level; while the expressions of downstream artemisinin pathway genes including *DBR2*, *ADS* and *CYP71AV1* were dramatically reduced, which catalyzed the formation of amorpha-4,11-diene and its ultimate conversion to DHAA (Figure 8 A). Interestingly, we observed a consistent result in the *TAR1*-OX lines, and the expressions of special enzyme genes involved in artemisinin biosynthesis were dramatically increased especially *ADS* and *CYP71AV1* by dozens and thousands of times, respectively (Figure 8B, 8C). These results indicate that TAR1 regulates the biosynthesis of artemisnin, probably by regulating the expression of key enzyme genes.

Some ERF subfamily proteins have been proved to specifically bind to GCC box (AGCCGCC). A recent study has shown that AaERF1 is able to bind to the GCC box *cis*-acting element (Zhu et al., 2014). To examine the binding activity of TAR1 to the GCC box, a GST fusion recombinant TAR1 protein was constructed and overexpressed in *E. coli* BL21 (Supplemental Figure 7) to examine the DNA binding ability by EMSA. The purified GST- TAR1 protein was mixed with the labeled 3× GCC probe or unlabeled competitor probe in the binding reaction. The results of EMSA showed that the gel mobility shift was specific to the GST-TAR1 protein with the labeled 3×GCC probe (Figure 9A, 9B). As expected, a reduced shifted band was detected when excess cold probe was added and no shifted band was observed in negative control (Figure 9B). The results demonstrate that TAR1 can specifically bind to GCC box which is consistent with the expectation of AP2/ERF TFs.

The CRTDREHVCBF2 (CBF2) and RAV1AAT (RAA) motifs present in both *ADS* and *CYP71AV1* promoters are often involved in the activation of these two genes. Previous work has demonstrated that the AP2/ERF TFs, sunch as AaERF1 and AaERF2, could directly bind to CBF2 and RAA (Yu et al. 2012). In this study, EMSA

was performed to test whether TAR1 has the ability to bind to the promoters of *ADS* and *CYP71AV1*. The recombinant protein of GST-TAR1 showed binding activities to both 3×CBF2 and 3×RAA fragments (Figure 9A, 9C and 9D). The DNA binding specificity was further confirmed in the competition experiments by addition of unlabeled probes as competitors. As shown in Figure 9C and 9D, the addition of excess CBF2 and RAA competitor DNAs reduced the formation of the complex. The labeled probe without fusion protein was used as negative control, and no complex was detected in this line. To further examine the binding activities of TAR1 to the promoters of *ADS* and *CYP71AV1*, yeast one-hybrid (Y1H) assays were performed. Triple repeated RAA, CBF2 motifs and their mutant nucleotide sequences were integrated into the genome of yeast cells, respectively. The combinations of pGAD-TAR1 and pHIS-CBF2 or pHIS-RAA were very strong compared with the blank pGAD or mutant CBF2, RAA motif (Figure 9E), which proved that TAR1 could directly bind to CBF2 and RAA motif.

To provide more evidence that TAR1 regulates the transcription of *ADS* and *CYP71AV1*, an *Agrobacterium*-mediated transient expression assay was performed. The promoter fragments (Supplemental Figure 8A-C) of *ADS* (~2.0 kb), *CYP71AV1* (~1.3 kb, Yu et al. 2011), *DBR2* (~1.7 kb, KC347592.1) and the mutated *ADS*, *CYP71AV1* promoters were used to drive the GUS reporter gene, respectively, and pCAMBIA-ADSpro:GUS, pCAMBIA-CYP71AV1pro:GUS, pCAMBIA-DBR2pro:GUS, pCAMBIA-mADSpro:GUS and pCAMBIA-mCYP71AV1pro:GUS were constructed. *TAR1* was overexpressed under the control of double 35S promoter (PHB-35S:TAR1). Each promoter-GUS construct was then transformed into *TAR1* overexpressed transgenic *A. annua* or co-transferred with *35S:TAR1* into wild-type *A. annua* leaves. Each promoter-GUS construct was transformed solely into wild-type *A. annua*, used as control. We found that TAR1 increased the GUS reporter gene expression both in *35S:TAR1* stably or transiently transformed *A. annua*, and the transiently overexpressed *TAR1* showed a stronger ability to activate the promoter of *ADS* and *CYP71AV1* (Figure 9F, 9G). These results support the hypothesis that TAR1 recognizes and interacts with the RAA and CBF2

palindromes present in *ADS* and *CYP71AV1* promoters, and activates the transcription of *ADS* and *CYP71AV1* in vivo. However, TAR1 can hardly activate the transcription of DBR2 and mutant *ADS* and *CYP71AV1* promoters (Supplemental Figure 8D). Therefore, *TAR1* is involved in a crucial regulation network controlling the biosynthesis of AR through regulating *CYP71AV1* and *ADS*.

## DISCUSSION

Malaria is a global health problem. In 2014, 97 countries and territories had ongoing malaria transmissions. An estimated 3.2 billion people are at risk of malaria, of whom 1.2 billion are at high risk (WHO, 2014). Isolated from the plant *A. annua*, or sweet wormwood, artemisinin and its derivatives are powerful medicines known for their ability to swiftly reduce the number of *Plasmodium* parasites in the blood of patients with malaria (WHO, 2014). Trichomes, divided into GSTs and TNGs, are small protrusions of epidermal origin on the surfaces of leaves and other organs of *A. annua* and many other plants. One of the most remarkable features of *Aa*GSTs is their capacity to synthesize, store and secrete artemisinin and many other specialized metabolites (Schilmiller et al., 2008, Olsson et al., 2009). However, relatively little is known about the regulation mechanism of artemisinin biosynthesis and the development of its specialized producer organ (*Aa*GSTs) and TNGs. Here, we report the characterization of *TAR1* as an essential gene for the yield of artemisinin and trichome formation in *A. annua*.

### TAR1 Is Essential for GSTs and TNGs Trichome Development in *A. annua*

GSTs are the site for the accumulation of artemisinin and other secondary metabolic products, so the correct development and formation of GSTs is vital for the yield of artemisinin. *TAR1* is expressed mainly in young tissues including young leaf, especially apical meristem, and early bud, and the expression is decreased as the leaves grow older. GUS staining of *pTAR1*-GUS transgenic plants showed that *TAR1* was expressed in TNGs trichomes and some GSTs cells (Figure 2). These results suggest that *TAR1* may participate in the initiation or formation development of GST

and TNG trichomes.

Production of artemisinin relies significantly on the right development and formation of its producer organ, GST trichomes. *Aa*GSTs are a 10-celled biseriate translucent structure of two stalk cells, two basal cells, four sub-apical cells and two apical cells (Duke et al., 1993; Olsson et al., 2009), and the biosynthesis of artemisinin takes place in both apical and sub-apical cells (Olofsson et al., 2012; Soetaert et al., 2013), which contain chloroplasts (Olsson et al., 2009). Artemisinin and other sesquiterpenoids (Duke et al., 1994; van Nieuwerburgh et al., 2006) as well as monoterpenoids (Tellez et al., 1999) are excreted into and stored in the subcuticular space. In *TAR1-RNAi A. annua*, many GSTs have an abnormally inflated top, with a cell number of six, (except two stalk cells which are usually embedded in the leaf), while the cell number of wild-type GST is eight (Figure 5A-5F). In addition, the autofluorescence of GSTs in *TAR1-RNAi* lines was very weak compared with the wild-type *Aa*GSTs (Figure 5G-5L). In accordance with the defective in GSTs, the content of artemisinin, AA and DHAA were all significantly reduced in different *TAR1-RNAi* lines (Figure 4). These results demonstrate a defect of GSTs in *TAR1-RNAi* plants, and suggest that *TAR1* gene is required for the normal development of GSTs.

TAR1 belongs to AP2/ERF TF family, which function as key regulators in plant metabolism and development. Moreover, AP2/ERF TF family is intensively studied TFs involved in cuticle development. Gain-of-function mutants of *WAX INDUCER1* (*WIN1*)/*SHINE1* (*SHN1*) from Arabidopsis and barley (*Hordeum vulgare*) have been reported (Aharoni et al., 2004; Kannangara et al., 2007; Taketa et al., 2008). The Arabidopsis overexpressing *WIN1*/*SHN1*, *SHN2*, or *SHN3* and *shn* gain-of-function mutant plants exhibit an increased accumulation of epidermal wax than wild type, ectopic wax crystals in leaves, and increased expression of genes involved in wax biosynthesis, including *ECERIFERUM1* (CER1), *3-KETOACYLCOA SYNTHASE1* (*KCS1*), and *CER2* (Aharoni et al., 2004; Broun et al., 2004; Oshima et al., 2013). In addition, *SHN* gene overexpression altered the leaf and petal epidermal cell structure, trichome number, and branching as well as the stomatal index. Because of the

changes in plant surface, the seedling of *35S:SHN1/WIN1* has hardly any trichomes on the adaxial side surface of first and second pairs of true leaves, and trichomes present on the first leaves of *35S:SHN1/WIN1* were nearly all single branched and located on leaf blade margins (Aharoni et al., 2004). In agreement with these AP2/ERF phylogenetic neighbors, the surface of *TAR1-RNAi A. annua* was changed as well with abnormal cuticular wax deposition and cuticle permeability as well as changed phenotype of TNGs (Figures 5-6). So far, only three *A. annua* genes involved in cuticular wax biosynthesis, including *TFAR*, *OSC2* and *CYP716A14v2*, have been identified. We find that the decreased accumulation of C24, C26-alco and α-amyrone coordinates with the reduced expression of *TFAR* and *CYP716A14v2* in *TAR1*-silenced plants. However, the content of β-amyrone is increased, possibly due to the redundant activity of the other β-amyrone synthase, just like the two β-amyrin synthase BAS and OSC2 (Moses et al., 2015). Therefore, TAR1 is critical for the normal development of not only GSTs but also TNGs.

**The *TAR1* Gene Is Involved in A Crucial Regulation Network Controlling the Biosynthesis of Artemisinin in *A. annua***

In *TAR1-RNAi* lines, the accumulation of artemisinin, AA and DHAA decreased in young leaves and buds compared with the same stage wild-type *A. annua*. Meanwhile, the transcription of genes involved in artemisinin biosynthesis including *ADS*, *CYP71AV1* and *DBR2* was down regulated too. On the contrary, the expressions of *DXR* and *DXS* were increased in the upstream reaction of plastidial MEP pathway, which was supposed to participate in the biosynthesis of monoterpenes, diterpenes, caroternoids, etc (Wu et al., 2012), while IPP mainly used for the biosynthesis of sequiterpenes and triterpenes was derived from the cytosolic MVA pathway (Figure 8). As expected, the expression of special genes involved in artemisinin biosynthesis pathway was dramatically increased in *TAR1*-OX *A. annua* (Figure 8B, 8C). Therefore, TAR1 may regulate the biosynthesis of artemisinin by regulating the genes involved in artemisinin biosynthesis pathway.

The AP2/ERF genes constitute a large multigene family, and members of AP2/ERF

TFs usually function as key regulators in plant metabolism, development and adaptive responses to environmental stimuli. As a member of AP2/ERF TF family, TAR1 is expected to recognize the *cis*-acting element AGCCGCC, known as GCC box (Hao et al., 1998; Zhang et al., 2009). EMSA experiment confirmed the binding activity of TAR1 to GCC box (Figure 9). In addition, the expressions of *ADS* and *CYP71AV1* were dramatically down-regulated in *TAR1-RNAi A. annua* according to the qRT-PCR result. Recently, two AP2/ERF TFs, AaERF1 and AaERF2, were proved to regulate two important enzymes (ADS and CYP71AV1) involved in artemisinin biosynthesis, by directly binding to the CBF2 and RAA motifs respectively (Yu et al. 2012). Similar with AaERF1 and AaERF2, TAR1 can also recognize and interact with the RAA and CBF2 palindromes present in *ADS* and *CYP71AV1* promoters, as demonstrated by the EMSA and yeast one-hybrid assays(Figure 9C-E). Furthermore, TAR1 activated the promoters of *ADS* and *CYP71AV1* in vivo (Figure 9F, 9G), but not the mutant *ADS, CYP71AV1* promoters or DBR2 promoter (Supplemental Figure 8D). Therefore, TAR1 may regulate the biosynthesis of artemisinin by regulating the transcription of *ADS* and *CYP71AV1* and as an important gene involved in crucial regulation network.

In conclusion, we have first demonstrated the role of TAR1, an AP2/ERF TF, in regulating both trichome development and artemisinin biosynthesis in *A. annua*. TAR1 is mainly expressed in young leaves, flower buds and some trichomes, and is localized within the cell nucleus. In *TAR1-RNAi A. annua*, the artemisinin production was reduced, the development of GSTs and TNGs was abnormal and the wax load and cuticle permeability were altered. When *TAR1* was overexpressed, the expression of *ADS* and *CYP71AV1* increased dramatically, as well as the content of artemisinin, AA and DHAA. Furthermore, TAR1 could directly bind to CBF2 and RAA motifs and activate the transcription of *ADS* and *CYP71AV1 in vivo*. Our findings suggest that the TAR1 protein may act as a key regulating molecule that controls the biosynthesis of artemisinin, the cuticular wax accumulation on cuticle and the development of trichomes. This work provides novel insights into the mechanism by which the biosynthesis of artemisinin is regulated and deepens the understanding of

AP2/ERF TFs and the development of trichomes, especially GSTs, which do not exist in Arabidopsis.

## METHODS

### Plant and Material

The *A. annua* seeds, obtained from the School of Life Sciences, Southwest University in Chongqing, China, were seeded directly on the soil and grown in a greenhouse with 12/12-h light/dark photoperiod at 26℃ for expression pattern analysis.

To gain sterilized seedlings, seeds of *A. annua* were surface-sterilized in 75% ethanol for 1 min and then in sodium hypochlorite solution with 1.7% active chlorine for 15min. After being rinsed five times thoroughly with sterile distilled water, the seeds were placed on Murashige and Skoog (MS) medium (Sigma-Aldrich, St Louis, MO, USA) plus 3% sucrose and 0.5% agar (pH 5.8).

### Spatial and Temporal Expression Analysis of *TAR1* by qRT-PCR

Total RNA was extracted using Trizol $A^+$ (Tiangen Biotech, Beijing, China) reagent, as described by the supplier, from different tissues, including root, stem, leaves, bud1, bud2 and flowers and from leaves at different position (counted from the apical top leave of the main stem). 1μg total RNA was used to synthesize the oligo (dT) primed first-strand cDNA using the TransScript First-strand cDNA Synthesis SuperMix kit (TransGen Biotech). Quantitative real-time RT–PCR (qRT–PCR) was performed with the SYBR-Green PCR Mastermix kit (Takara) on a Thermal Cycler Dice. Expression levels were normalized to those of the Actin control gene (EU531837). For organ-specific expression, all tissues were collected from at least four plants grown in the field for 6 months. For expression dynamics analysis, all leaves were collected from four plants grown to a height of 45-55 cm. The experiments were repeated in triplicate. All the primers for RT-PCR are listed in Supplemental Table 1 online (Lu et al., 2013).

### Subcellular Localization Analysis of TAR1-GFP Fusion Proteins

To investigate the subcellular localization of *TAR1*, the encoding region without the stop codon of *TAR1* was cloned into the *Nco* I and *Spe* I sites of *pCAMBIA1301* vector

fused with GFP in-frame under the control of the cauliflower mosaic virus 35S promoter. The final vector, *TAR1-GFP*, was used for transient expression in rice protoplast cells. GFP fluorescent signals were imaged at the excitation wavelength of 488 nm and emission wavelength of 505–530 nm. The red autofluorescence of chlorophylls was imaged at emission wavelength longer than 650 nm (Shi et al., 2011).

**Fluorescence Micrographs of Leaves in Transgenic Lines Expressing *pTAR1:TAR1-GFP***

To from the *pTAR1-GFP*, the 1.36-kb upstream region of the TAR1 gene was cloned into the *Bam* HI and *Nco* I sites of *pCAMBIA1301:GFP* to substitute the 35S promoter. *TAR1*, with *Nco* I and *Spe* I sites, was cloned into the *pTAR1:GFP* construct to form the final vector p*TAR1:TAR1-GFP*. Then, the construct was transformed into *A. annua* plant by *Agrobacterium* (Zhang et al., 2009). For the in vivo subcellular localization analysis of TAR1, leaves of wild type and *pTAR1:TAR1-GFP* transgenic plant were examined by A laser scanning confocal microscope (Leica TCS SP5) as described previously (Tan et al., 2012).

**GUS Expression and Staining in Transgenic *A. annua***

To construct *pTAR1-GUS*, the 1360-bp upstream region of TAR1 was amplified from genomic DNA using the Genome Walker Kit (Clontech, Mountain View, CA, USA). The 5'-flanking DNA of the *TAR1* coding region was generated with specific primers (TAR1pro-F, TAR1pro-R) and subcloned into *pCAMBIA1301:GUS* by *Bam* HI and *Nco* I sites. *pTAR1-GUS* was transformed into *A. annua* as described previously. Histochemical staining for GUS activity in transgenic plants was performed as modified reference (Jefferson et al., 1987).

**Construction of *TAR1* RNAi Vector and *A. annua* Transformation**

A 414-bp fragment of *TAR1* containing the 184th to 597th nucleotides, was PCR-amplified for RNAi constructs. TAR1i-F (with *Nco* I and *Xba* I sites) and TAR1i-R (with *Bam* HI and *Kpn* I sites) were used as the forward and reverse primers, respectively. The modified *pC1300-pHANNIBAL* vector constructed by our lab with a 35S promoter, a PDK intron and an OCS terminal from *pHANNIBAL* was used as the

RNAi vector. The fragment was placed in forward (digested with *Nco* I and *Kpn* I) and reverse (digested with *Bam* HI and *Xba* I) orientation on the two ends of the PDK intron to generate the *1300-pHANNIBAL-TAR1-RNAi* construct. Then the construct was transformed into wild-type *A. annua* via *Agrobacterium* EHA105-mediated transformation. *A. annua* transformed with *pC1300-pHANNIBAL* empty vector were used as control. More than three independent lines were tested in these experiments including gene expression, determination of wax and artemisinin and phenotype observation.

**Construction of *TAR1* Overexpression Vector and *A. annua* Transformation**

The full-length coding region of *TAR1* was amplified from leaves cDNA with primers PHB-TAR1-F and PHB-TAR1-R. Then the fragment was inserted into the *Bam* HI and *Spe* Ⅰ sites of modified binary vector *PHB-Flag* under the control of two 35S promoter to form the final construct. The construct was transferred into *Agrobacterium* EH105, and finally introduced into *A. annua*. The plants that were transformed with *PHB-Flag* were used as control. At least three independent lines were tested in these experiments including gene expression and metabolism detection.

**Liquid Chromatography Tandem Mass Spectrometry**

Buds of *A. annua* were dried at 45°C and pestled into fine powder, extracted with 1.5ml ethanol /0.1g sample. The suspension was supersonic for 30 min and then centrifuged at 5 000 rpm for 10 min to remove the suspended particles (Lu et al., 2013). The final supernatant was filtered through a 0.25um pore size filter. Contents of artemisinin, AA and DHAA were determined by Liquid Chromatography Tandem Mass Spectrometry (LC-MS/MS).

LC-MS/MS analysis was run on an Agilent 1200 infinity LC coupled with an Agilent 6410 Triple Quadrupole LC/MS System (Agilent, USA). The LC operating conditions were as follows: LC column, ZORBAX SB-C18, 2.1×100mm i.d., 3.5 μm silica; mobile phase, Acetonitrile - 0.1% formic acid (70:30); total flow rate of mobile phase, 0.3 ml/min; total run time including equilibration, 4.2 min. The injection volume was 5 μl. The MS/MS was operated with electrospray ionization (ESI) source in the positive ion mode with multiple reaction monitoring (MRM). The nebulizer gas

pressure was set at 40 psi with the source temperature of 350℃ and the gas flow at 10 L/min. The capillary voltage was 4000 V (positive mode). High-purity nitrogen gas was used as collision cell gas. The raw chromatograph and mass spectrogram data were processed with the MassHunter Workstation software (Agilent, USA).

**Epicuticular Wax Extraction and Chemical Analysis**

A total of 100–200 mg of fresh leaves from transgenic *A. annua* was pooled and epicuticular wax was exhaustively extracted with 5 ml of chloroform for 5 min at room temperature. The solution was filtered through a 0.22um pore size filter and then dried under a gentle stream of nitrogen. The resulting residues was transmethylated and silylated with 75 μL MSTFA:TMCS (99:1) in 75 μL pyridine to transform all hydroxyl-containing compounds into the corresponding trimethylsilyl derivatives. The samples were derivatized at 70°C for 1 h and then n-Heptane (100 mL) was added to dilute the solution. The solution was centrifuged at 5 000 rpm for 10 min and the final supernatant was used for GC-MS analysis. Tricosane (C23; yeyuan, China) was added as internal standard after derivatization, to a final concentration of 100 μg/mL injected.

The qualitative composition was studied with a Thermo-Finnigan Trace DSQ fasting scanning single-quadrupole MS (Thermo Electron Corporation) operated at unit mass resolving power. A 1.0 μL sample solution was injected with splitless mode to TB-5MS column (30 m×250 μm ×0.25 μm) with helium as the carrier gas at a flow of 1.0 mL/min. The temperature profile was 50℃ oven for 2 min, raised by 40℃/min to 200℃, held for 2 min at 200℃, then raised again by 2℃/min to 235℃ and held for 5 min at 235℃, finally from 235℃ to 310℃ at 3℃/min and held for 5min.

**Electrophoretic Mobility Shift Assay**

Full-length of TAR1 was inserted into the expression vector pGEX-4T-1 between the *Bam* HI and *Xho* I sites to increase protein solubility. The recombinant TAR1 protein was expressed in *Escherichia coli* and purified according to the Bio-Rad instruction manual. The probe sequences were triple tandem copies of the CRTAREHVCBF2 (CBF2) motif, RAV1AAT (RAA) motif and GCC-BOX synthesized by sheng gong as shown in Table S1. All of them were labeled with biotin on 3’ ends. Y-CBF2-F and

Y-CBF2-R were annealing to form double-nucleic acids of CBF2 motif probe. Y-RAV-F and Y-RAV-R were annealing to form double-nucleic acids of RAA motif probe. Y-GCC-F and Y-GCC-R were annealing to form double-nucleic acids of GCC-box probe.

**Yeast One-Hybrid Assay**

To analyze the binding activity of TAR1 protein, the ORF of TAR1 was fused into the *Bam* HI and *Xho* I sites of the activation domain of the pGADT7 vector (pGAD) to form the prey. The sequences containing the CBF2 and RAA motif were inserted into pHIS2 with *EcoR* I and *Sac* I sites to generate baits, respectively. Moreover, the mutant CBF2 motif ("G" to "T") and RAA motif ("C" to "T") sequences were inserted into pHIS2 by same enzymes as negative control baits. The prey and baits constructs were co-transformed into yeast strain Y187. The positively transformed clones were grown on SD/-Leu-Trp-His medium with 30mM of 3-amino-1,2,4-triazole (3-AT) for 3 days at 30℃. Two kind of negative yeasts were co-transformed by pGADT7-TAR1 and mutant pHIS-mCBF2 or mRAA as well as pGADT7 and pHIS-CBF2 or RAA. All the sequences were synthesized by sheng gong as shown in Table S1.

**Transient Expression Assay in *A. annua***

For the construct of recombinant expression vector, the promoters of ADS，CYP71AV1 (Yu et al. 2012) and DBR2 (KC347592.1) were amplified from the *A. annua* genome by PCR with the primers (pADS-F and R, pCYP71AV1-F and R, pDBR2-F and R) list in supplementary table 1. With an *Xba* I sticky end (5') and a *Nco* I sticky end (3'), the 2094 bp long ADS promoter, 1304 bp CYP71AV1 promoter and 1725bp DBR2 promoter (Supplemental Figure 8) were inserted into the pCAMBIA1301 vector, generating pCAMBIA-ADSpro:GUS, pCAMBIA-CYP71AV1pro:GUS and pCAMBIA-DBR2pro:GUS. Moreover, the mutant ADS and CYP71AV1 promoters (change "G" to "T" in CBF2 motif and "C" to "T" in RAA motif, Supplemental Figure 8, synthesized by genewiz company) were cloned into pCAMBIA1301 vector, forming pCAMBIA-mADSpro:GUS and pCAMBIA-mCYP71AV1pro:GUS constructs. To form the *TAR1* overexpression

vector, the ORF of *TAR1* was inserted into the binary vector PHB-flag between *Bam* HI and *Spe* Ⅰ sites under the control of two 35S promoters. After this, pCAMBIA-ADSpro:GUS and *TAR1* overexpression plasmid were co-introduced into wild-type *A. annua* plant or the pCAMBIA-ADSpro:GUS alone was introduced into *TAR1* overexpression transgenic *A. annua* by *Agrobacterium*-mediated transformation respectively, and the transient transformation of *A. annua* were performed as previously described by Ma et al., 2009. In the same way, each pro:GUS was introduced into wild-type and transgenic *A. annua* respectively.

## SUPPLEMENTARY DATA

Supplementary Data are available at Molecular Plant Online.

*FUNDING*

This work was supported by funds from the National Natural Science Foundation of China (Grant no. 31300159, 31160059, 31300257 and 81325024); "Pujiang Talent" program (13PJ1411000) and "Rising Star" program (14QB1402700) from Shanghai Science and Technology Committee.

**Figure Legends**

**Figure 1. Molecular Identification and Phylogenetic Analysis of TAR1.**

(A) A schematic representation of the exon and intron organization of *TAR1*. +1 indicates the starting nucleotide of translation, and the stop codon (TAG) is +543. Black boxes indicate exons, intervening lines indicate introns, the gray box indicates the 5' and 3'-untranslated region and the white box indicates the AP2 domain.

(B) A protoplast expressing free GFP showing the green fluorescence in the cytosol.

(C) A protoplast that expressed TAR1-GFP showing fluorescence in the nucleus.

(D) The same protoplast of (C) showing the red chlorophyll autofluorescence signal.

(E) The same protoplast of (C) under white light. Bars=5μm.

(F) Bootstrap neighbor-joining phylogenetic tree was constructed using MEGA and 1000 replicates. The proteins are named according to their gene names or NCBI accession numbers. Three AP2 transcriptors of *A. annua* are defined as outgroup. The length of the branches refers to the amino acid variation rates. The alignment on which the tree was constructed is shown in Supplemental Figure S1 online.

(G) The deduced amino acid sequence of TAR1 is compared with the sequences of *AtWIN1*, *AtSHINE3*, *AaERF1* and *AaERF2*. AP2 domain is boxed. Black boxes indicate identical residues and gray boxes indicate similar residues.

**Figure 2. The Expression Pattern of *TAR1*.**

(A) Spatial expression analyses of *TAR1* by semi-quantitative RT-PCR. *Actin* (EU531837) and GDNA (genomic DNA) was served as control. OL, old leaf, YL, young leaf;

(B) qRT-PCR analysis of *TAR1* expression in different tissues. *Actin* was used as a control for normalization. Each data point is the average of three biological repeats. Error bars indicate Standard Deviations (SD).

(C) A schematic diagram of *A. annua* plant show the sampling point of (D). L, leaf.

(D) The temporal expression of *TAR1* by semi-quantitative RT-PCR in different development stage leaves. *Actin* and GDNA (genomic DNA) was served as control.

(E) qRT-PCR analysis of *TAR1* expression in different development stage leaves. *Actin* was used as a control for normalization. Each data point is the average of three biological repeats. Error bars indicate SD.

(F-G) GUS expression (blue staining) patterns in the leaves of *pTAR1-GUS* transgenic lines. (F) Show the young leaf. (G) Show the leaf apical meristem.

(H) A negative control, GUS staining in young leaf of wild-type *A. annua*.

(I-K) GUS expression in GSTs of the *pTAR1-GUS* transgenic line leaf. S, stalk cells; B, basal cells; Sa, sub-apical cells; A, apical cells.

(L) GUS expression in TNGs of the *pTAR1-GUS* transgenic line leaf.

(M) GUS staining in the flower buds of *pTAR1-GUS* transgenic line.

(N) A negative control, showing the GUS staining in flower buds of wild-type *A. annua*.

Bars=50 μm in (F-H); =100 μm in (M-N); =10 μm in (I-L).

**Figure 3. Localization Analysis of TAR1-GFP.**

(A) Diagrams of *pTAR1: TAR1-GFP* constructs. 1.3-kb 5' upstream sequence of *TAR1* was used as the promoter to drive gene expression.

(B-F) Fluorescence micrographs of leaf cells in transgenic lines expressing *pTAR1: TAR1-GFP*. (E) is superimposed from GFP (green) and DAPI (blue). (F) is superimposed from GFP, DAPI and chlorophyll autofluorescence (red).

(G-K) The leaf of wild type *A. annua* serves as the negative control. Bars=50 μm.

**Figure 4. Contents of Artemisinin, Artemisinic acid and Dihydroartemisinic acid in *TAR1* silenced and overexpressed *A. annua.***

(A) Diagrams of *TAR1* RNA interference construct *1300-pHANNIBAL-TAR1-RNAi*. 414bp not conservative sequence of *TAR1* was used.

(B) The structures of Artemisinin, Artemisinic acid and Dihydroartemisinic acid, respectively.

(C) LC-MS/MS analysis of Artemisinin, Artemisinic acid and Dihydroartemisinic acid in leaves (upper panel) and buds (lower panel) of different *TAR1*- RNAi lines.

Each data point is the average of three biological replicates. Bars indicate SD. Level of significance obtained with a Student's t test marked by the following: *, $P < 0.05$; ⁑, $P < 0.01$.

(D) LC-MS/MS analysis of Artemisinin, Artemisini c acid and Dihydroartemisinic acid in leaves (upper panel) and buds (lower panel) of different *TAR1* overexpression lines. Each data point is the average of three biological replicates. Bars indicate SD. Level of significance obtained with a Student's t test marked by the following: *, $P < 0.05$; ⁑, $P < 0.01$. OX, overexpression.

**Figure 5. Phenotypic Analysis of *TAR1-RNAi A. annua*.**

(A-C) The surface of wild type (A) and *TAR1-RNAi* plants (B-C) leaf dealt with 75% ethanol and observed using light microscopy.

(D-F) The surface of wild type (D) and *TAR1-RNAi* plants (E-F) leaf treat with phosphate buffer overnight, decolorized by 75% alcohol and observed under light microscopy. Red arrows, normal GSTs; blue arrows, abnormal GSTs.

(G-L) The adaxial surface observed using fluorescence microscopy of leaves derived from Wild type (G, H) and *TAR1-RNAi* plants (I-L). White arrows, normal GSTs; blue arrows, abnormal GSTs; black arrows, TNGs.

Bars=50 μm in (A-F); =500 μm in (G-L).

**Figure 6. SEM Analysis of The Leaf Surface of Wild Type and *TAR1-RNAi A. annua*.**

(A-B) Scanning electron microscopy (SEM) image of adaxial surface of wild type (A) and *TAR1-RNAi* (B) *A. annua* leaves.

(C-F) Detail of wild type (C and E) and *TAR1-RNAi* (D and F) leaves showing leaf surface and the abnormal extended, distorted and filiform TNGs.

(G-H) SEM images of adaxial side leaf from wild type (G) and *TAR1-RNAi* (H) plants. Surface of *TAR1-RNAi* leaf is covered with abnormal wax deposition, whereas wild-type surface is smooth and shows only little wax deposition. Bars=500 μm in (A-B); =100 μm in (C-D); =50 μm in (E-F); =10 μm in (G-H).

**Figure 7. The Cuticle Permeability and Three Major Cuticular Wax Fractions of Wild-Type and *TAR1-RNAi A. annua* Leaves.**

(A) Chlorophyll extracted in 80% ethanol for 2 h from leaves of *TAR1-RNAi* lines compared with empty vector control leaves.

(B) Chlorophyll leaching assays with leaves of *TAR1-RNAi* lines and empty vector control lines immersed in 80% ethanol for different time intervals. The results are derived from three independent experiments and depicted with standard error of the mean for each time point. fw, fresh weight.

(C) Quantitative analysis of C24, C26 and C28 fatty alcohol components in wild type and *TAR1* RNAi transgentic lines. alco, fatty alcohol. Each data point is the average of three biological replicates. Bars indicate SD. Level of significance obtained with a Student's t test marked by the following: *, $P < 0.05$; **, $P < 0.01$.

(D) Quantitative analysis of C16, C18, C20 and C22-dio fatty acid components in wild type and *TAR1-RNAi* lines. acid, fatty acid.

**Figure 8. Gene expression of Artemisinin Biosynthetic pathway in *TAR1- RNAi* and *TAR1* Overexpression *A. annua*.**

(A) qRT-PCR analyses of artemisinin biosynthetic genes in wild type and *TAR1-RNAi* plants. *Actin* was used as a control for normalization. Each data point is the average of three technical repeats and the results were consistent in three biological replicates. Error bars indicate SD.

(B) qRT-PCR analyses of artemisinin biosynthetic genes in wild type and *TAR1* overexpression plants. OX, overexpression.

(C) The artemisinin biosynthetic pathway showing the up regulatied (red) genes of upstream MEP pathway and down regulatied (blue) genes of artemisinin biosynthesis pathway in *TAR1-RNAi* plant. The abbreviations were described in supplementary data.

**Figure 9. Binding Assay of *TAR1* to GCC, RAA and CBF2 *cis*-Elements, and the Activation of *ADS* and *CYP71AV1* Promoters by *TAR1*.**

(A) The sequences of oligonucleotides used in Electrophoretic mobility shift assay (EMSA), possessing triple GCC-box, CBF2 motif and RAA motif respectively. The key nucleotides were underlined.

(B) EMSA binding analysis of TAR1 protein to triple GCC boxes. Lane 1: GST-TAR1fusion protein plus Cy5-labelled GCC probe; lane 2: the binding of GST-TAR1fusion protein and Cy5-GCC probe compete by 10-fold concentration cold probes; lane 3: negative control contain only Cy5-GCC probe.

(C, D) EMSA binding analysis of TAR1 protein to triple CRTDREHVCBF2 (CBF2) and triple RAV1AAT (RAA) *cis*-elements. Four micrograms GST-TAR1fusion protein were incubated with 7μg Cy5-labeled CBF2(C) or RAA (D) at 25℃ for 20 min. 10x, 10-fold molar excess of unlabeled probe; red arrows, shifted probe; blue arrows, free probe.

(E) Yeast one-hybrid assay for the interaction between TAR1 protein with CBF2 and RAA motifs. Triple CBF2 motif, RAA motif and mutant CBF2, RAA motif were used as bait respectively. Yeast cells carrying pGAD-TAR1and pHIS-CBF2 or pHIS RAA were grown on SD/-Leu-Trp-His medium with 30mM of 3-AT. Blank pGAD or mutant CBF2, RAA motif were used as negative controls. Cells were spotted as one-tenth dilutions.

(F) Transactivation of *ADSpro:GUS* gene expression by TAR1 in *A. annua* leaves. qRT–RCR analysis of the GUS gene expression in transiently transformed or *35s:TAR1*stably transgenic *A. annua* with *Agrobacterium* harboring *ADSpro:GUS* and *35s:TAR1* or *ADSpro:GUS* alone.

(G) Transactivation of *CYP71AV1pro:GUS* gene expression by TAR1 in *A. annua.* qRT–RCR analysis of the GUS gene expression in transiently transformed or *35s:TAR1* stably transgenic *A. annua* with *Agrobacterium* harboring *CYP71AV1pro:GUS* and *35s:TAR1* or *CYP71AV1pro:GUS* alone.

Table1. Composition of Cuticular Wax on Leaves of the Wild Type and the *TAR1* silenced lines.

| Compound class | Wild type (WT) (µg/g) n=3 | *TAR1-RNAi* lines (µg/g) n=4 | Average reduction (%) |
|---|---|---|---|
| Fatty acids | 1141.81 ± 57.43 | 876.83 ± 43.97 | 23..20* |
| Primary alcohols | 201.32 ± 27.40 | 169.01 ± 27.65 | 16.05 |
| Alkanes | 2775.26 ± 129.79 | 1989.21 ± 100.29 | 28.32** |
| Esters | 96.50 ± 28.48 | 77.25 ± 14.67 | 19.94 |
| Terpenes | 130.97 ± 7.54 | 119.31 ± 9.76 | 8.90 |
| Total | 8547.16 ± 588.83 | 6352.88 ± 358.96 | 25.67* |

The coverage of total extracted lipids and of individual compound classes are given as mean values with standard deviation. Level of significance obtained with a Student's t test marked by the following: *, $P < 0.05$; **, $P < 0.01$.

## *REFERENCES*

**Aharoni, A., Dixit, S., Jetter, R., Thoenes, E., van Arkel, G., and Pereira, A.** (2004). The SHINE clade of AP2 domain transcription factors activates wax biosynthesis, alters cuticle properties, and confers drought tolerance when overexpressed in Arabidopsis. Plant Cell. **16,** 2463-2480.

**Broun, P., Poindexter, P., Osborne, E., Jiang, C.Z., and Riechmann, J.L.** (2004). WIN1, a transcriptional activator of epidermal wax accumulation in Arabidopsis. Proc. Natl. Acad. Sci. USA **101,** 4706-4711.

**Covello, P.S.** (2008). Making artemisinin. Phytochemistry. **69,** 2881-2885.

**Crespo-Ortiz, M.P., and Wei, M.Q.** (2012). Antitumor Activity of Artemisinin and Its Derivatives: From a Well-Known Antimalarial Agent to a Potential Anticancer Drug. Journal of Biomedicine and Biotechnology **2012,** 18.

**Duke, M.V., Paul, R.N., Elsohly, H.N., Sturtz, G., and and Duke, S.O.** (1994). Localization of Artemisinin and Artemisitene in Foliar Tissues of Glanded and Glandless Biotypes of *Artemisia annua* L. International journal of plant science. **155,** 365-372.

**Duke, S.O., and Paul, R.N.** (1993). Development and fine structure of the glandular trichomes of *Artemisia annua* L. International journal of plant science **154,** 107-118.

**Efferth, T., Romero, M.R., Wolf, D.G., Stamminger, T., Marin, J.J., and Marschall, M.** (2008). The antiviral activities of artemisinin and artesunate. Clin. Infect. Dis. **47,** 804-811.

**Ferreira, J.F.S., and Janick, J.** (1995). Floral Morphology of *Artemisia annua* with Special Reference to Trichomes. International journal of plant science **156,** 807-815.

**Graham, I.A., Besser, K., Blumer, S., Branigan, C.A., Czechowski, T., Elias, L., Guterman, I., Harvey, D., Isaac, P.G., Khan, A.M., Larson, T.R., Li, Y., Pawson, T., Penfield, T., Rae, A.M., Rathbone, D.A., Reid, S., Ross, J., Smallwood, M.F., Segura, V., Townsend, T., Vyas, D., Winzer, T., and Bowles, D.** (2010). The genetic map of *Artemisia annua* L. identifies loci affecting yield of the antimalarial drug artemisinin. Science **327,** 328-331.

**Jefferson, R.A., Kavanagh, T.A., and Bevan, M.W.** (1987). GUS fusions: beta-glucuronidase as a sensitive and versatile gene fusion marker in higher plants. EMBO J. **6,** 3901-3907.

**Kannangara, R., Branigan, C., Liu, Y., Penfield, T., Rao, V., Mouille, G., Hofte, H., Pauly, M., Riechmann, J.L., and Broun, P.** (2007). The transcription factor WIN1/SHN1 regulates Cutin

biosynthesis in *Arabidopsis thaliana*. Plant cell **19,** 1278-1294.

**Licausi, F., Ohme-Takagi, M., and Perata, P.** (2013). APETALA2/Ethylene Responsive Factor (AP2/ERF) transcription factors: mediators of stress responses and developmental programs. New Phytol. **199,** 639-649.

**Lu, X., Zhang, L., Zhang, F., Jiang, W., Shen, Q., Zhang, L., Lv, Z., Wang, G., and Tang, K.** (2013). AaORA, a trichome-specific AP2/ERF transcription factor of *Artemisia annua*, is a positive regulator in the artemisinin biosynthetic pathway and in disease resistance to Botrytis cinerea. New phytol. **198,** 1191-1202.

**Ma, D., Pu, G., Lei, C., Ma, L., Wang, H., Guo, Y., Chen, J., Du, Z., Wang, H., Li, G., Ye, H., Liu, B.** (2009). Isolation and characterization of AaWRKY1, an Artemisia annuatranscription factor that regulates the amorpha-4,11-diene synthase gene, a keygene of artemisinin biosynthesis. Plant Cell Physiol. 50,2146–61.

**Maes., L., Nieuwerburgh., F.C.W.V., Zhang., Y., Reed., D.W., Pollier., J., Casteele., S.R.F.V., Inze., D., Covello., P.S., and Goossens., D.L.D.D.a.A.** (2011). Dissection of the phytohormonal regulation of trichome formation and biosynthesis of the antimalarial compound artemisinin in *Artemisia annua* plants. New Phytol. **189,** 176–189.

**Moses T, Pollier J, Shen Q, Soetaert S, Reed J, Erffelinck ML, Van Nieuwerburgh FC, Vanden Bossche R, Osbourn A, Thevelein JM, Deforce D, Tang K, Goossens A.** (2015) OSC2 and CYP716A14v2 Catalyze the Biosynthesis of Triterpenoids for the Cuticle of Aerial Organs of Artemisia annua. Plant Cell. 27(1), 286-301.

**Nguyen, K.T., Arsenault, P.R., and Weathers, P.J.** (2011). Trichomes + roots + ROS = artemisinin: regulating artemisinin biosynthesis in *Artemisia annua* L. In Vitro Cell Dev. Biol. Plant. **47,** 329-338.

**Noorden, R.V.** (2010). Demand for malaria drug soars. Nature **466,** 672-673.

**Okamuro, J.K., Caster, B., Villarroel, R., Van Montagu, M., Jofuku, K.D.** (1997). The AP2 domain of APETALA2 defines a large new family of DNA binding proteins in Arabidopsis. Proc Natl Acad Sci U S A. 94(13), 7076-81.

**Olofsson, L., Lundgren, A., and Brodelius, P.E.** (2012). Trichome isolation with and without fixation using laser microdissection and pressure catapulting followed by RNA amplification: Expression of genes of terpene metabolism in apical and sub-apical trichome cells of

*Artemisia annua* L. Plant Sci. **183,** 9-13.

**Olofsson, L., Engstrom, A., Lundgren, A., and Brodelius, P.E.** (2011). Relative expression of genes of terpene metabolism in different tissues of *Artemisia annua* L. BMC Plant Biol. **11,** 45.

**Olsson, M.E., Olofsson, L.M., Lindahl, A.L., Lundgren, A., Brodelius, M., and Brodelius, P.E.** (2009). Localization of enzymes of artemisinin biosynthesis to the apical cells of glandular secretory trichomes of *Artemisia annua* L. Phytochemistry. **70,** 1123-1128.

**Oshima, Y., Shikata, M., Koyama, T., Ohtsubo, N., Mitsuda, N., and Ohme-Takagi, M.** (2013). MIXTA-like transcription factors and WAX INDUCER1/SHINE1 coordinately regulate cuticle development in Arabidopsis and Torenia fournieri. Plant Cell. **25,** 1609-1624.

**Sakuma, Y., Liu, Q., Dubouzet, J.G., Abe, H., Shinozaki, K., Yamaguchi-Shinozaki, K.** (2002). DNA-binding specificity of the ERF/AP2 domain of Arabidopsis DREBs, transcription factors involved in dehydration- and cold-inducible gene expression. Biochem Biophys Res Commun. 290(3), 998-1009.

**Schilmiller, A.L., Last, R.L., and Pichersky, E.** (2008). Harnessing plant trichome biochemistry for the production of useful compounds. Plant J. **54,** 702-711.

**Shi, J., Tan, H., Yu, X.H., Liu, Y., Liang, W., Ranathunge, K., Franke, R.B., Schreiber, L., Wang, Y., Kai, G., Shanklin, J., Ma, H., and Zhang, D.** (2011). Defective pollen wall is required for anther and microspore development in rice and encodes a fatty acyl carrier protein reductase. Plant Cell. **23,** 2225-2246.

**Soetaert, S.S., Van Neste, C.M., Vandewoestyne, M.L., Head, S.R., Goossens, A., Van Nieuwerburgh, F.C., and Deforce, D.L.** (2013). Differential transcriptome analysis of glandular and filamentous trichomes in *Artemisia annua*. BMC Plant Biol. **13,** 220.

**Taketa, S., et al.** (2008). Barley grain with adhering hulls is controlled by an ERF family transcription factor gene regulating a lipid biosynthesis pathway. Proc. Natl. Acad. Sci. USA. 105, 4062–4067.

**Tan, H., Liang, W., Hu, J., and Zhang, D.** (2012). MTR1 encodes a secretory fasciclin glycoprotein required for male reproductive development in rice. Dev. Cell. **22,** 1127-1137.

**Tellez, M.R., Canel, C., Rimando, A.M., Duke, S.O.** (1999). Differential accumulation of isoprenoids in glanded and glandless *Artemisia annua* L. Phytochemistry. 52, 1035–1040.

**Teoh, K.H., Polichuk, D.R., Reed, D.W., and Covello, P.S.** (2009). Molecular cloning of an aldehyde

dehydrogenase implicated in artemisinin biosynthesis in *Artemisia annua*. Botany **87,** 635-642.

**Teoh, K.H., Polichuk, D.R., Reed, D.W., Nowak, G., and Covello, P.S.** (2006). *Artemisia annua* L. (Asteraceae) trichome-specific cDNAs reveal CYP71AV1, a cytochrome P450 with a key role in the biosynthesis of the antimalarial sesquiterpene lactone artemisinin. FEBS Lett. **580,** 1411-1416.

**van Nieuwerburgh, F.C.W., Vande Casteele, S.R.F., Maes, L., Goossens, A., Inzé, D., van Bocxlaer, J., Deforce, D.L.D.** (2006). Quantitation of artemisinin and its biosynthetic precursors in *Artemisia annua* L. by high performance liquid chromatography–electrospray quadrupole time-of-flight tandem mass spectrometry. J. Chromatogr. A. 1118, 180–187.

**Wang, H., Han, J., Kanagarajan, S., Lundgren, A., and Brodelius, P.E.** (2013). Trichome-specific expression of the amorpha-4,11-diene 12-hydroxylase (cyp71av1) gene, encoding a key enzyme of artemisinin biosynthesis in *Artemisia annua*, as reported by a promoter-GUS fusion. Plant Mol. Biol. **81,** 119-138.

**Wang, Y.Y., Yang, K., Jing, F.Y., Li, M.Y., Deng, T., Huang, R.Z., Wang, B.S., Wang, G.F., Sun, X.F., and Tang, K.X.** (2011). Cloning and characterization of trichome-specific promoter of cpr71av1 gene involved in artemisinin biosynthesis in *Artemisia annua* L. Mol. Biol. **45,** 751-758.

**Wang, Z., Qiu, J., Guo, T.B., Liu, A., Wang, Y., Li, Y., and Zhang, J.Z.** (2007). Anti-Inflammatory Properties and Regulatory Mechanism of a Novel Derivative of Artemisinin in Experimental Autoimmune Encephalomyelitis. J. Immunol. **179,** 5958-5965.

**World Health Organization**. (2014) World Malaria Report 2014. http://www.who.int/malaria/media/world_malaria_report_2014/en/

**Wu, T., Wang, Y., and Guo, D.** (2012). Investigation of glandular trichome proteins in *Artemisia annua* L. using comparative proteomics. PloS one **7,** e41822.

**Xu H, Zhang F, Liu B, Huhman DV, Sumner LW, Dixon RA, Wang G.** (2013) Characterization of the formation of branched short-chain fatty acid:CoAs for bitter acid biosynthesis in hop glandular trichomes. Mol Plant. 6(4), 1301-17.

**Yu, Z.X., Li, J.X., Yang, C.Q., Hu, W.L., Wang, L.J., and Chen, X.Y.** (2012). The jasmonate-responsive AP2/ERF transcription factors AaERF1 and AaERF2 positively regulate artemisinin biosynthesis in *Artemisia annua* L. Mol. Plant. **5,** 353-365.

**Zhang, G., Chen, M., Li, L., Xu, Z., Chen, X., Guo, J., Ma, Y.** (2009). Overexpression of the soybean GmERF3 gene, an AP2/ERF type transcription factor for increased tolerances to salt, drought, and diseases in transgenic tobacco. J Exp Bot. 60(13), 3781-96.

**Zhang F., Fu X., Lv Z., Lu X., Shen Q., Zhang L., Zhu M., Wang G., Sun X., Liao Z., and Tang K.** (2015). A Basic Leucine Zipper Transcription Factor, AabZIP1, Connects Abscisic Acid Signaling with Artemisinin Biosynthesis in *Artemisia annua* L. Mol. Plant. 8, 163–175.

**Zhang, L., Jing, F., Li, F., Li, M., Wang, Y., Wang, G., Sun, X., and Tang, K.** (2009). Development of transgenic *Artemisia annua* (Chinese wormwood) plants with an enhanced content of artemisinin, an effective anti-malarial drug, by hairpin-RNA-mediated gene silencing. Biotechnol. Appl. Biochem. **52,** 199-207.

**Zhu, D., Wu, Z., Cao G., Li, J., Wei, J., Tsuge T., Gu H., Aoyama, T., Qu, L.J.** (2014) *TRANSLUCENT GREEN*, an ERF family transcription factor, controls water balance in Arabidopsis by activating the expression of aquaporin genes. Mol. Plant. 7(4), 601-15.